

The Dirac Quantum Cellular Automaton in one dimension: Zitterbewegung and scattering from potential

Alessandro Bisio,^{*} Giacomo Mauro D’Ariano,[†] and Alessandro Tosini[‡]
*Dipartimento di Fisica dell’Università di Pavia, via Bassi 6, 27100 Pavia and
 Istituto Nazionale di Fisica Nucleare, Gruppo IV, via Bassi 6, 27100 Pavia*

We study the dynamical behaviour of the quantum cellular automaton of Refs. [1, 2], which reproduces the Dirac dynamics in the limit of small wavevectors and masses. We present analytical evaluations along with computer simulations, showing how the automaton exhibits typical Dirac dynamical features, as the Zitterbewegung and the scattering behaviour from potential that gives rise to the so-called Klein paradox. The motivation is to show concretely how pure processing of quantum information can lead to particle mechanics as an emergent feature, an issue that has been the focus of solid-state, optical and atomic-physics quantum simulator.

PACS numbers: 03.67.Ac, 03.67.Lx, 03.65.Pm

I. INTRODUCTION

The idea of reproducing the evolution of a macroscopic system starting from a simple rule of local interaction among its elementary constituents was first formalized in the pioneering von Neumann’s paper [3] with the notion of *Cellular Automaton*. The automaton is a regular lattice of cells with a finite number of states, equipped with a rule that updates the cell states from time t to time $t + 1$. Such rule must be *local*, namely the state of the x cell at $t + 1$ depends only on the states of a finite number of neighboring cells at t . Cellular automata have been a popular topic for many years, as a new paradigm for complex systems, and many books have been devoted to the subject (see eg. Refs. [4, 5]). One of the reasons of its first success, which eventually has become its own weakness, is the chaotic behaviour of the automaton dynamics [6].

Differently from classical cellular automata, *Quantum Cellular Automata* (QCA) exhibit a less chaotic behaviour, which makes them predictable for large number of steps [7]. Here the cells are finite-dimensional quantum systems interacting locally and unitarily. Being locality of interactions an essential ingredient of any physical evolution, QCA have been considered already by Feynman as candidates for simulating physics [8, 9]. More recently QCA earned interest in the quantum information community leading to many results on its mathematical theory [10–12], and on their general dynamical features [7, 13–16]. In quantum field theory, after the first appearance of a prototype of QCA in the Feynman chessboard [8] for solving the path-integral for the Dirac field, a similar framework has appeared in the work of Nakamura [17] motivated by a rigorous formulation of the Feynman path integral, and later in the seminal work

of Bialynicki-Birula [18], as a lattice theory for Weyl, Dirac, and Maxwell fields. Then the possibility of using automata for describing the evolution of relativistic fields emerged in the context of lattice-gas simulations, especially in the work of Meyer [19], where a notion of “field automaton” first appeared, and in the papers of Yepez [20].

More recently QCA have been considered for extending quantum field theory [1] to the Planck scale. Similar to lattice-gas theories, here the quantum cell corresponds to the evaluation $\psi(x)$ of a quantum field on the site x of a lattice, with the dynamics updated in discrete time steps by a local unitary evolution. However, differently from lattice-gas theory, here the continuum limit is not taken, whereas, instead, the asymptotic large-scale (Fermi) evolution is considered. The main difference is then that Lorentz covariance holds exactly in the relativistic limit of small momentum, whereas generally it is distorted, in a fashion analogous to Refs. [21–23]. In this context the one dimensional Dirac automaton has been derived from symmetry principles for the QCA [2] showing how the usual Dirac dynamics emerges at the Fermi scale, though relativistic covariance and other symmetries are violated at the Planck/ultrarelativistic scale.

In the present paper we analyze in detail the one-particle sector of the automaton of Refs. [1, 2]. Here, particle states are “smooth” states peaked around a momentum eigenstate of the QCA. We will consider dynamical quantities as the particle position, momentum and velocity, along with their evolution both in the free case and in the presence of a potential, recovering typical features of Dirac quantum field evolution—as *Zitterbewegung* and *Klein paradox*—from the pure quantum information processing of the QCA. Recently there has been a renewed interest in Dirac features in solid-state and atomic physics, which provide a physical hardware to simulate the dynamics. Zitterbewegung can be seen in the response of electrons to external fields [24] and can appear for nonrelativistic particles in a crystal [25–27], quasiparticles in superconductors [28] and systems with spin-orbit coupling [29, 30]. Proving that the oscillation behavior is

^{*}alessandro.bisio@unipv.it

[†]dariano@unipv.it

[‡]alessandro.tosini@unipv.it

not unique to Dirac electrons, but rather is a generic feature of spinor systems with linear dispersion relations, these works opened the way for possible simulation of Zitterbewegung using for example trapped ions [31, 32], two-band crystalline structure such as graphene [33, 34] or semiconductors [35–39], ultra cold atoms [40], and finally photonic crystals [41]. On the other hand, the Klein paradox (tunneling of relativistic particles) provides insight in the mechanics of relativistic particles propagating through potential barriers, along with vacuum polarization effects, and has been a focus in the hot topic of graphene as a simulator for Dirac equation, as in Ref. [42], and [32] for trapped ions. Recently also microfabricated optical waveguide circuits have become an alternative physical simulator for particle dynamics [43].

After reviewing the Dirac QCA in 1d in Section II, in Section III we present the evolution of position and momentum operators for the automaton, showing the Zitterbewegung behaviour produced by the interference between positive and negative frequencies. In Section IV we modify the QCA in order to insert a potential in the free evolution, and show the automaton dynamics in the presence of a barrier for one particle states.

We end the paper with a summary and some concluding remarks in Section V.

II. THE DIRAC AUTOMATON

The quantum automaton corresponding to the Dirac equation in 1d, first introduced in [1], has been derived from the discrete automaton symmetries of parity and time-reversal in Ref. [2], where also the Dirac equation has been recovered as the large-scale relativistic limit of the automaton. The cell of the quantum automaton is given by the evaluation $\psi(x)$ of the two-component field operator ψ , and the unitary evolution of one step of the automaton is given by

$$\psi(x) \rightarrow U\psi(x), \quad \psi(x) := \begin{pmatrix} \psi_r(x) \\ \psi_l(x) \end{pmatrix} \quad (1)$$

where ψ_l and ψ_r denote the *left* and *right* mode of the field, whereas the unitary matrix U is given by

$$U = \begin{pmatrix} nS & -im \\ -im & nS^\dagger \end{pmatrix}, \quad n^2 + m^2 = 1, \quad (2)$$

with S denoting the shift operator $Sf(x) = f(x+1)$. The constants n and m in the last equation can be chosen positive. As shown in Refs. [1, 2], the parameter m plays the role of an a -dimensional inertial mass, and is bounded by unit. We remark that the automaton description is completely a -dimensional, and a conversion to the usual physical dimensions needs a length, a time and a mass, which one can take as the Planck length ℓ_P , the Planck time τ_P , and the Planck mass m_P , the latter playing the role of the bound for the inertial mass. The maximal speed of propagation of information is one cell

per step ($c = \ell_P/\tau_P$ in dimensional units, corresponding to the speed of light). The quantum field can be taken generally as Fermionic, Bosonic, or even Anyonic. However, in the present case it will not be relevant, since we will consider only single-particle states, which span the Hilbert space $\mathbb{C}^2 \otimes l_2(\mathbb{Z})$, and for which we will use the factorized orthonormal basis $|s\rangle|x\rangle$, where for $|s\rangle$ we consider the canonical basis corresponding to $s = l, r$. These states can be also obtained as $\psi_s^\dagger(x)|\Omega\rangle$ upon introducing a vacuum $|\Omega\rangle$ which is annihilated by the field operator, and invariant under the automaton evolution. Similarly also N -particle states with $N > 1$ can be obtained by acting with products of N evaluations of the field operator, building up the Fock space in the usual way. Notice that the evolution of the field is restricted to be linear, and there exists a unitary operator U such that the field evolution is given by $V\psi_s(x)V^\dagger = U\psi_s(x)$, with $V|\Omega\rangle = |\Omega\rangle$, whereas for product of field evaluations the evolution is given by tensor powers of U as $V\psi_{s_1}(x_1)\dots\psi_{s_N}(x_N)V^\dagger = U^{\otimes N}\psi_{s_1}(x_1)\otimes\dots\otimes\psi_{s_N}(x_N)$.

In the $|s\rangle|x\rangle$ representation the unitary matrix U can be written as follows

$$U := \sum_x \begin{pmatrix} n|x-1\rangle\langle x| & -im|x\rangle\langle x| \\ -im|x\rangle\langle x| & n|x+1\rangle\langle x| \end{pmatrix}, \quad (3)$$

describing a *Quantum Walk* on the Hilbert space $\mathbb{C}^2 \otimes l_2(\mathbb{Z})$ [7].

Tanks to the translational invariance of U , it is convenient to move to the momentum representation

$$|\psi_s\rangle|k\rangle := \frac{1}{\sqrt{2\pi}} \sum_x e^{-ikx} |\psi_s\rangle|x\rangle, \quad k \in [-\pi, \pi], \quad (4)$$

and U becomes

$$U = \int_{-\pi}^{\pi} dk U(k) \otimes |k\rangle\langle k|, \quad U(k) = \begin{pmatrix} ne^{ik} & -im \\ -im & ne^{-ik} \end{pmatrix}. \quad (5)$$

Notice that discreteness bound momenta to the Brillouin zone, as in solid-state theory. By diagonalizing the unitary matrix $U(k)$

$$U(k)|s\rangle_k = e^{-is\omega(k)}|s\rangle_k, \quad \omega(k) = \arccos(n \cos k) \quad (6)$$

$$|s\rangle_k := \frac{1}{\sqrt{2}} \begin{bmatrix} \sqrt{1-sv(k)} \\ s\sqrt{1+sv(k)} \end{bmatrix}, \quad s = \pm, \quad v(k) := \partial_k \omega(k)$$

it is easy to evaluate the logarithm of U ($e^{-iH} := U$) as follows

$$H = \int_{-\pi}^{\pi} dk H(k) \otimes |k\rangle\langle k|, \quad (7)$$

$$\begin{aligned} H(k) &= \omega(k) (|+\rangle_k \langle +|_k - |-\rangle_k \langle -|_k) \\ &= \text{sinc}^{-1}\omega(k) (-n \sin k \sigma_3 + m \sigma_1), \end{aligned}$$

where σ_i $i = 1, 2, 3$ denote the usual Pauli matrices.

The function $\omega(k)$ is the dispersion relation of the automaton, which recovers the usual Dirac one $\omega(k) =$

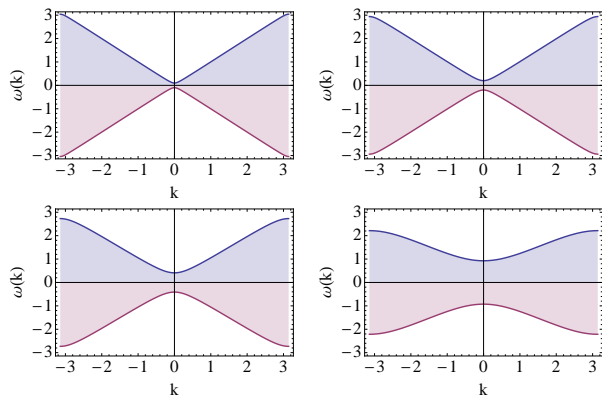


FIG. 1: The Dirac automaton dispersion relation in Eq. (6) for four different values of the mass: $m = 0.1, 0.2, 0.4, 0.8$.

$\sqrt{k^2 + m^2}$ in the limit $k, m \ll 1$ and $k/m \gg 1$ as shown in [2]. This is also clear in Fig. 1 where the dispersion relation as a function of k is reported for four different values of the mass. The derivative $v(k)$ in Eq. (6) is then the group velocity of the wavepacket. The $s = +1$ eigenvalues correspond to positive-energy particle states, whereas the negative $s = -1$ eigenvalues correspond to negative-energy anti-particle states.

Notice that the operator H regarded as an Hamiltonian would interpolate the evolution to continuous time as $U(t) \equiv U^t$, which, however, in this context should be considered unphysical [49]

In the following sections we will analyze two typical aspects of the Dirac-field dynamics, namely the Zitterbewegung and the Klein paradox.

III. POSITION AND MOMENTUM OPERATORS AND ZITTERBEWEGUNG

The QCA (2) describes very precisely the Dirac field dynamics for customary relativistic wavevectors and energies (consider that e.g. a ultra-high-energy cosmic ray has $k \simeq 10^{-8}$) [2]. In this section we will show how efficiently it reproduces a typical feature of the one-particle Dirac dynamics, namely the Zitterbewegung.

The Zitterbewegung was first recognized by Schrödinger in 1930 [44] who noticed that in the Dirac equation describing the free relativistic electron the velocity operator does not commute with the Dirac Hamiltonian: the evolution of the position operator, in addition to the classical motion shows a very fast periodic oscillation with frequency $2mc^2$ and amplitude equal to the Compton wavelength \hbar/mc with m the rest mass of the relativistic particle. This jittering motion first encountered in the Dirac theory of the electron was then shown [24] to arise from the interference of states corresponding to the positive and negative energies resulting from the Dirac equation with the trembling disappearing with time [45] for a wavepacked particle state. Zitterbewegung oscillations cannot be directly

observed by current experimental techniques for a Dirac electron since the amplitude should be very small $\approx 10^{-12}$ m. However, it can be seen in a number of solid-state, atomic-physics, photonic-crystal and optical waveguide simulators, as quoted in the introduction.

The “position” operator X providing the representation $|x\rangle$ (i.e. such that $X|s\rangle|x\rangle = x|s\rangle|x\rangle$) is defined as follows

$$X = \sum_{x \in \mathbb{Z}} x (I \otimes |x\rangle\langle x|). \quad (8)$$

Generally X provides the average location of a wavepacket in terms of $\langle \psi | X | \psi \rangle$. The conjugated “momentum” operator is given by

$$P = \int_{-\pi}^{\pi} \frac{dk}{2\pi} k (I \otimes |k\rangle\langle k|). \quad (9)$$

One can verify that X and P obey the usual canonical commutation rule $[X, P] = i$. In the following it will be convenient to work with the continuous time t interpolating exactly the discrete automaton evolution, namely U^t . However, all numerical results will be given only for discrete t , namely for repeated applications of the automaton unitary U in Eq. (2).

The time evolution of the position operator $X(t) = U^{-t} X U^t$ can be more easily computed by integrating the differential equation $A(t) = [H, [H, X(t)]]$ where H was defined in Eq. (7). We have

$$\begin{aligned} A(t) &= \int_{-\pi}^{\pi} dk A(k, t) \otimes |k\rangle\langle k| \quad A(k, t) = e^{2iH(k)t} A(k) \\ A(k) &= -\frac{2\omega^2}{\sin^2 \omega} nm \cos k \sigma_2 \end{aligned} \quad (10)$$

which leads to

$$X(t) = X(0) + Vt + Z_X(t) - Z_X(0) \quad (11)$$

$$V(k) = -v(k)^2 \sigma_3 + v(k) \sqrt{1 - v(k)^2} \sigma_1 \quad (12)$$

$$Z_X(k, t) = -\frac{1}{4} H^{-2}(k) A(k, t) \quad (13)$$

where V is the classical component of the velocity operator which, in the base diagonalizing the Hamiltonian (7), is $V(k) = v(k) \sigma_3$ and is proportional to the group velocity $v(k)$. Since a generic one-particle state $|\psi\rangle$ is a superposition of a positive and a negative energy state, i.e. $|\psi_+\rangle + |\psi_-\rangle$, the evolution of the mean value of the position operator $X(t)$, can be written as

$$\begin{aligned} x_\psi(t) &:= \langle \psi | X(t) | \psi \rangle = x_\psi^+(t) + x_\psi^-(t) + x_\psi^{\text{int}}(t) \\ x_\psi^\pm(t) &:= \langle \psi_\pm | X(0) + Vt | \psi_\pm \rangle \\ x_\psi^{\text{int}}(t) &:= 2\Re[\langle \psi_+ | X(0) - Z_X(0) + Z_X(t) | \psi_- \rangle] \end{aligned} \quad (14)$$

where \Re denotes the real part. The interference between positive and negative frequency is responsible of the $x_\psi^{\text{int}}(t)$. The magnitude of $x_\psi^{\text{int}}(t)$ is bounded by $1/m$

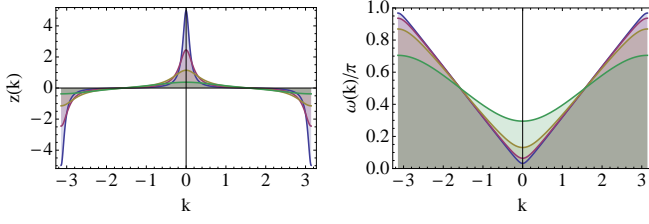


FIG. 2: (Colors online) Plots of $z(k)$ (left) and $\omega(k)/\pi$ (right) related to the oscillation amplitude and frequency of the position expectation value in Eq. (11). In both cases the plots are reported for different values of the mass ($m = 0.1, 0.2, 0.4, 0.8$ from the top in the figure on the left and from the bottom in the figure on the right).

(see appendix A) which in the usual dimensional units correspond to the Compton wavelength \hbar/mc . Moreover the stationary phase approximation shows that for $t \rightarrow \infty$ the term $2\Re[\langle\psi_+|Z_X(t)|\psi_-\rangle]$, which is responsible of the oscillation, goes to 0 as $1/\sqrt{t}$ (see appendix A) and only the shift contribution coming from $2\Re[\langle\psi_+|X(0) - Z_X(0)|\psi_-\rangle]$ survives. These results show that $x_\psi^{\text{int}}(t)$ is the automaton analogue of the so-called Zitterbewegung. As already noticed in the introduction this phenomenon was never observed for a free relativistic electron because of the small value of $x_\psi^{\text{int}}(t)$ which is bounded by the electron Compton wave length 10^{-12} m in natural units. The results of this section are in agreement with the one for the Hadamard walk [46].

In Fig. 3 we have considered the evolution of states with particle and antiparticle components smoothly peaked around some momentum eigenstate, namely

$$c_+|\psi_+\rangle + c_-|\psi_-\rangle, \quad |\psi_\pm\rangle = \int \frac{dk}{\sqrt{2\pi}} g_{k_0}(k) |\pm\rangle_k |k\rangle \quad (15)$$

where $c_+^2 + c_-^2 = 1$ and g_{k_0} is a Gaussian peaked around the momentum k_0 with width σ . An easy computation shows that for these states the shift contribution reduces to $2\Re[\langle\psi|X(0) + Z_X(0)|\psi\rangle] = \Im(c_+^*c_-)/(2\pi) \int_{-\pi}^{\pi} dk |g_{k_0}(k)|^2 z(k)$ with the function $z(k) = m \cos \omega(k)/\sin^2 \omega(k)$ bounded again by the Compton wavelength $1/m$ and the oscillation frequency given by $\omega(0)/\pi$ (see also Fig. 2).

IV. EVOLUTION WITH A SQUARE POTENTIAL BARRIER

In order to study the scattering with a potential, we modify the automaton adding a position dependent phase representing a square potential barrier, as in Refs. [46, 47]. We will provide explicitly the transmission T and reflection R coefficients as functions of the energy and mass of the incident wavepacket and of the potential barrier's height. We will find a general behavior independently on the regime, namely on the energy and mass

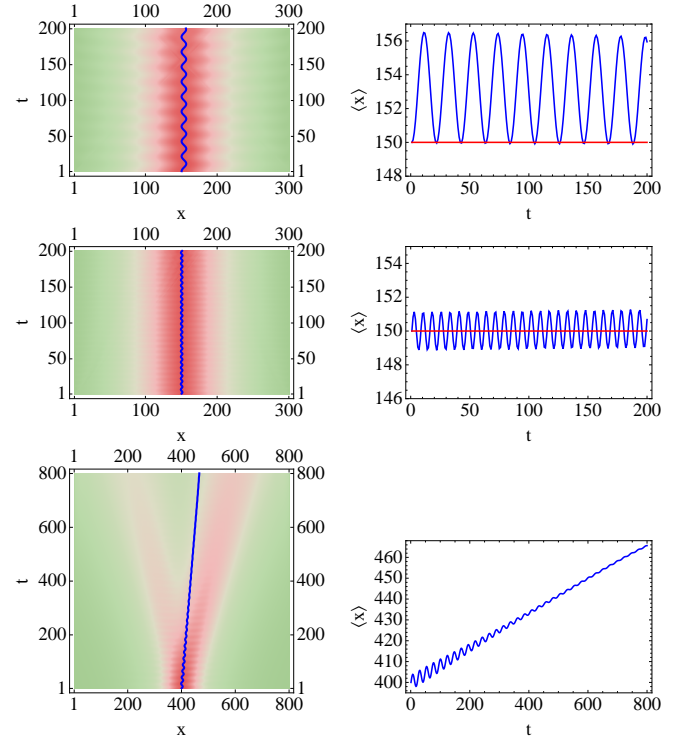


FIG. 3: Automaton evolution of a state as in Eq.(15) showing the Zitterbewegung of the position expectation value. **Top:** $m = 0.15, c_+ = 1/\sqrt{2}, c_- = i/\sqrt{2}, k_0 = 0$, and $\sigma = 40^{-1}$. The calculated shift and oscillation frequency are respectively $\langle\psi|X(0) + Z_X(0)|\psi\rangle = 3.2$ and $\omega(0)/\pi = 0.05$, accordingly to the simulation. **Middle:** $m = 0.15, c_+ = 1/\sqrt{2}, c_- = 1/\sqrt{2}, k_0 = 0, \sigma = 40^{-1}$. The calculated shift and oscillation frequency are 0 and 0.13, respectively. **Bottom:** $m = 0.13, c_+ = \sqrt{2/3}, c_- = 1/\sqrt{3}, k_0 = 10^{-2}\pi, \sigma = 40^{-1}$. In this case the particle and antiparticle contribution are not balanced and the average position drift velocity is thus $\langle\psi_+|V|\psi_+\rangle + \langle\psi_-|V|\psi_-\rangle = (|c_+|^2 - |c_-|^2)v(k_0) = 0.08$, corresponding to an average position $x_\psi^+(800) + x_\psi^-(800) = 464$ (see Eq. (14)). Notice that for $t \rightarrow \infty$ the term $2\Re[\langle\psi_+|Z_X(t)|\psi_-\rangle]$, which is responsible of the oscillation, goes to 0.

of the incident particle. Increasing the value of the potential barrier beyond a certain threshold a transmitted wave reappears and the reflection coefficient starts decreasing. The width of the $R = 1$ region is an increasing function of the mass which is proportional to the gap between positive and negative frequency eigenvalues of the unitary evolution.

For a generic potential $\phi(x)$, the unitary evolution becomes

$$U_\phi := \sum_x e^{-i\phi(x)} \begin{pmatrix} n|x-1\rangle\langle x| & -im|x\rangle\langle x| \\ -im|x\rangle\langle x| & n|x+1\rangle\langle x| \end{pmatrix}.$$

We will analyze the simple case $\phi(x) := \phi\theta(x)$ ($\theta(x)$ is the Heaviside step function) that is a potential step which is 0 for $x < 0$ (region I) and has a constant value $\phi \in [0, 2\pi]$ for $x \geq 0$ (region II) as illustrated in Fig. 4.

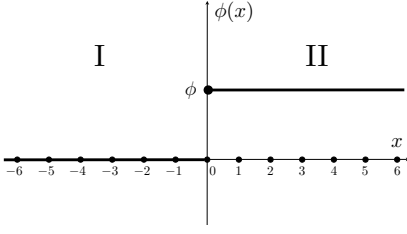


FIG. 4: Schematic of the potential

Let us now study the eigenvector of U_ϕ of the form

$$|\Phi_k\rangle = \Pi_I |+\rangle_k |k\rangle + \Pi_I \beta_k |+\rangle_{-k} |k\rangle + \gamma_k \Pi_{II} |+\rangle_{k'} |k'\rangle$$

$$\Pi_I := \sum_{x < 0} I \otimes |x\rangle \langle x| \quad \Pi_{II} := \sum_{x \geq 0} I \otimes |x\rangle \langle x|$$

where β_k , γ_k and k' are functions of k . The condition that $|\Phi_k\rangle$ is genuinely an eigenstate of U_ϕ , i.e. $U_\phi |\Phi_k\rangle = e^{-i\omega(k)} |\Phi_k\rangle$, implies that

$$\begin{aligned} \omega(k') &= \omega(k) - \phi \\ \beta_k &= \frac{e^{-ik} \sqrt{(1+v)(1-v')} - e^{-ik'} \sqrt{(1-v)(1+v')}}{-e^{ik} \sqrt{(1-v)(1-v')} + e^{-ik'} \sqrt{(1+v)(1+v')}} \\ \gamma_k &= \frac{2e^{i\xi}(v \cos k - i \sin k)}{-e^{ik} \sqrt{(1-v)(1-v')} + e^{-ik'} \sqrt{(1+v)(1+v')}} \end{aligned} \quad (16)$$

with $v := v(k)$ and $v' := v(k')$ the group velocities of the incident and transmitted wave. Let us now consider the superposition

$$|\Psi(0)\rangle := \int \frac{dk}{\sqrt{2\pi}} g_{k_0}(k) |\Phi_k\rangle$$

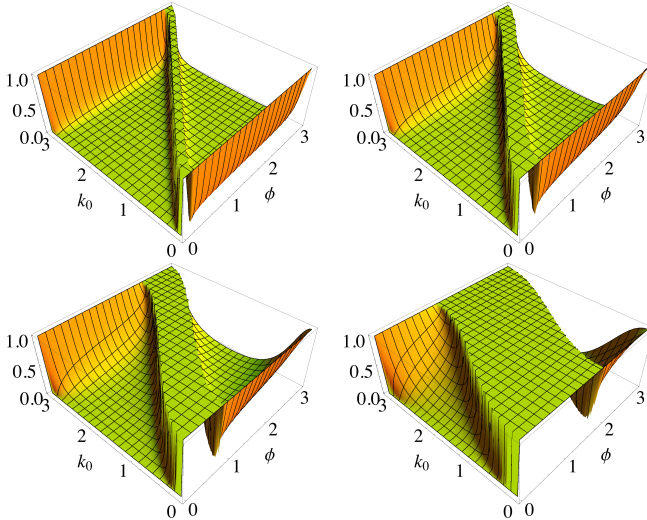


FIG. 5: Reflection coefficient as a function of the potential barrier height ϕ and of the momentum k of the incident particle state. From the top-left to the bottom-right the reflection coefficient is depicted for different values of the mass: $m = 0.1, 0.2, 0.4, 0.8$.

where $g_{k_0}(k)$ is a function in $C_0^\infty[-\pi, \pi]$ which we assumed to be smoothly peaked around k_0 . The state at time t is then

$$|\Psi(t)\rangle := \int \frac{dk}{\sqrt{2\pi}} g_{k_0}(k) e^{-i\omega(k)t} |\Phi_k\rangle$$

and one can verify that for $t \ll 0$ the state is negligible in region II while the only appreciable contribution in region II comes from the term $e^{ik_0 x}$ which describes a wavepacket that moves at group velocity $v(k_0)$ and hits the barrier from the left. When $t \gg 0$ the state can be approximated by a superposition of a reflected and a transmitted wavepacket as follows

$$\begin{aligned} |\Psi(t)\rangle &\xrightarrow{t \gg 0} \beta(k_0) \int \frac{dk}{\sqrt{2\pi}} g_{k_0}(k) e^{-i\omega(k)t} |+\rangle_{-k} |k\rangle + \\ &+ \tilde{\gamma}(k_0) e^{-i\phi t} \int \frac{dk}{\sqrt{2\pi}} \tilde{g}_{k'_0}(k') e^{-i\omega(k')t} |+\rangle_{k'} |k'\rangle \end{aligned}$$

where we defined

$$k'_0 \text{ s.t. } \omega(k'_0) = \omega(k_0) - \phi,$$

$$\tilde{\gamma}(k_0) := \gamma(k_0) \sqrt{\frac{v(k'_0)}{v(k_0)}}, \quad \tilde{g}_{k'_0}(k') = \sqrt{\frac{v(k'_0)}{v(k_0)}} g_{k'_0}(k')$$

(one can check $\int \frac{dk}{\sqrt{2\pi}} |\tilde{g}_{k'_0}(k')|^2 = 1$), whose group velocities are $-v(k_0)$ for the reflected wave packet and $v(k'_0)$ for the transmitted wave packet (see Fig. 6).

The probability of finding the particle in the reflected wavepacket is $R = |\beta(k_0)|^2$ (reflection coefficient) while the probability of finding the particle in the transmitted wavepacket is $T = |\tilde{\gamma}(k_0)|^2$ (transmission coefficient).

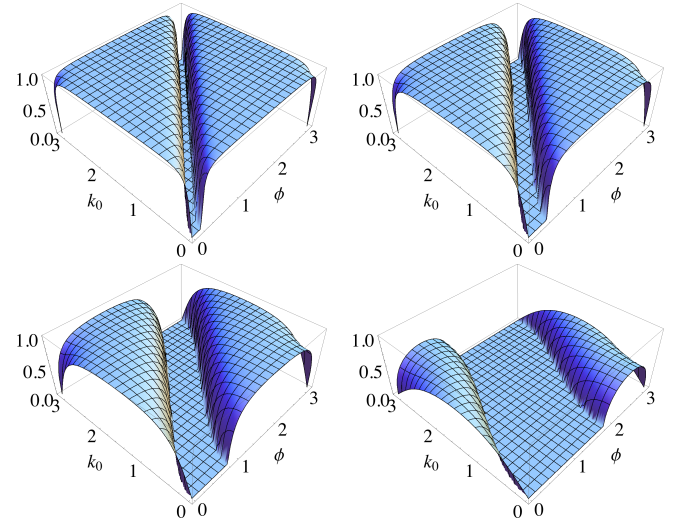


FIG. 6: Group velocity of the transmitted wave packet as a function of the potential barrier height ϕ and of the momentum k of the incident particle state. From the top-left to the bottom-right the transmitted group velocity for different values of the mass: $m = 0.1, 0.2, 0.4, 0.8$.

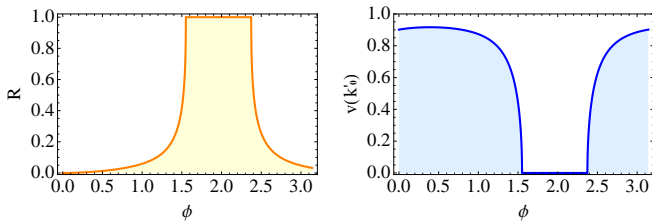


FIG. 7: Reflection coefficient for $m = 0.4$ and momentum of the incident particle $k_0 = 2$ as a function of the potential barrier height ϕ (section of plots in Figs. 5-6 for $m = 0.4$, $k_0 = 2$).

The consistency of the result can be verified by checking that $R + T = 1$. For $k \ll m \ll 1$ (Schrödinger regime) we recover the usual reflection and transmission coefficient for the Schrödinger equation with a potential step. In Fig. 5 we plot the reflection coefficient R as a function of ϕ and k for different values of the mass m . Clearly when $\phi = 0$ we have $R = 0$ and increasing ϕ while fixing k the value increases up to $R = 1$. One notice that when $\omega(k) - \arccos(n) < \phi < \omega(k) + \arccos(n)$ Eq. (16) has solution for imaginary k' which implies an exponential damping of the transmitted wave and pure reflection. By further increasing the value of ϕ beyond the threshold $\omega(k) + \arccos(n)$, Eq. (16) have solution for real k' and negative $\omega(k')$, and then a transmitted wave reappears and the reflection coefficient decreases. This is the so called “Klein paradox” which is originated by the presence of positive and negative frequency eigenvalues of the unitary evolution. The width of the $R = 1$ region is an increasing function of the mass equal to $2\arccos(n)$ which is the gap between positive and negative frequency solution solutions (see Fig. 1).

In Fig. 7 we plot the reflection R coefficient and the transmitted wave velocity group $v(k'_0)$ as a function of the potential barrier height ϕ with the incident wave packet having $k_0 = 2$ and $m = 0.4$. From the figure it is clear that after a plateau with $R = 1$ the reflection coefficient starts decreasing for higher potentials. In Fig. 8 we show the scattering simulation for four increasing values of the potential, say $\phi = 1.42, 1.55, 2, 2.4$ (see the caption to figure for the details).

V. CONCLUSIONS

In this paper we studied the dynamics of the quantum cellular automaton of Refs. [1, 2], which gives the Dirac dynamics as emergent in the limit of small wavevectors. We presented computer simulations and analytical evaluations, focusing on typical features of the Dirac dynamics, in particular the Zitterbewegung and the scattering from potential. Our automaton covers all regimes of masses and energy-momenta, beyond the same validity range of the Dirac equation, with the possibility of considering arbitrary input states, enabling to inves-

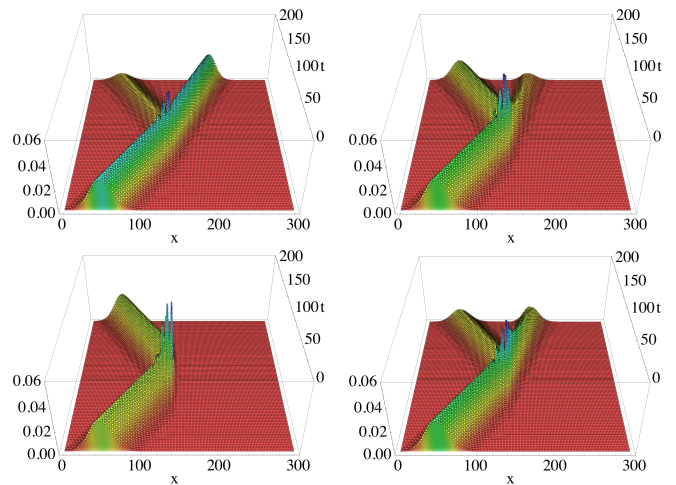


FIG. 8: Simulations of the Dirac automaton evolution with a square potential barrier. Here the automaton mass is $m = 0.2$ while the barrier turns on at $x = 140$. In the simulation the incident state is a smooth state of the form $|\psi(0)\rangle = \int \frac{dk}{\sqrt{2\pi}} g_{k_0}(k) |+\rangle_k$ peaked around the positive energy eigenstate $|+\rangle_{k_0}$ with $k_0 = 2$ and with g_{k_0} a Gaussian having width $\sigma = 15^{-1}$. The incident group velocity is $v(k_0) = 0.90$. The simulation is run for four increasing values of the potential ϕ . **Top-Left:** Potential barrier height $\phi = 1.42$, reflection coefficient $R = 0.25$, velocity of the transmitted particle $v(k'_0) = 0.63$. **Top-Right:** $\phi = 1.55$, $R = 0.75$, $v(k'_0) = 0.1$. **Bottom-Left:** $\phi = 2$, $R = 0.1$, $v(k'_0) = 0$. **Bottom-Right:** $\phi = 2.4$, $R = 0.50$, $v(k'_0) = 0.33$.

tigate and visualize a wide range of fundamental processes. This facts, in addition to the discreteness of the automaton, makes of it the ideal theoretical counterpart for the experimental simulators in the literature. A similar quantum cellular automaton can be also developed in two dimensions [48], corresponding to the graphene as quantum simulator.

Appendix A: Bound of the oscillating term and its asymptotic behavior

Here we provide an upper bound for the oscillating term $x_\psi^{\text{int}}(t)$ in Eq. (14) in the position operator evolution derived in Section III and we derive its behaviour for very long time steps. The jittering of the position expectation value is caused by the operator $Z_X(t)$ which in the base diagonalizing the automaton Hamiltonian H (7) can be written as

$$Z_X(t) = \int_{-\pi}^{\pi} dk e^{2i\omega(k)\sigma_z t} Z_X(k) \otimes |k\rangle\langle k|,$$

$$Z_X(k) = z(k)\sigma_2, \quad z(k) = \frac{m \cos \omega(k)}{2 \sin^2 \omega(k)}$$

with $z(k) \in L^1(-\pi, \pi)$ for any $m \neq 0$. By defining

$$|\psi_{\pm}\rangle = \int_{-\pi}^{\pi} \frac{dk}{\sqrt{2\pi}} g_{\pm}(k) |\pm\rangle_k |k\rangle, \quad g_{\pm}(k) \in C_0^{\infty}[-\pi, \pi]$$

we have

$$2\Re[\langle\psi_+|Z_X(t)|\psi_-\rangle] = \int_{-\pi}^{\pi} \frac{dk}{\pi} z(k) \Re\left[ig_+^*(k)g_-(k)e^{2i\omega(k)t}\right]$$

Since, for any $m \neq 0$, $\omega(k)$ has three stationary points in $k = 0, \pm\pi$ ($\omega^{(1)}(0) = \omega^{(1)}(\pm\pi) = 0$ and $\omega^{(1)}(k) \neq 0$ elsewhere in the closed interval $k \in [-\pi, \pi]$, with $\omega^{(2)}(0), \omega^{(2)}(\pm\pi) \neq 0$), the stationary phase approximation gives

$$2\Re[\langle\psi_+|Z_X(t)|\psi_-\rangle] \xrightarrow{t \gg 0} \sum_{k=0, \pm\pi} z(k) \Re\left[ig_+^*(k)g_-(k)e^{2i\omega(k)t} \sqrt{\frac{i}{\pi\omega^{(2)}(k)t}}\right]$$

showing that the term $2\Re[\langle\psi_+|Z_X(t)|\psi_-\rangle]$, goes to 0 as $1/\sqrt{t}$.

In order to find an upper bound for $x_{\psi}^{\text{int}}(t)$ notice that

$$\begin{aligned} |x_{\psi}^{\text{int}}(t)| &\leq 2|\langle\psi_+|X(0) - Z_X(0) + Z_X(t)|\psi_-\rangle| \\ &\leq 2(|\langle\psi_+|X(0)|\psi_-\rangle| + |Z_X(0)| + |Z_X(t)|) \end{aligned}$$

and, according to the expression of $Z_X(k)$, we get

$$\begin{aligned} |Z_X(0)| + |Z_X(t)| &\leq 2|Z_X(0)| \\ |Z_X(0)| &\leq \max_{k \in [-\pi, \pi]} |z(k)| = z(0) = \frac{\sqrt{1-m^2}}{2m}. \end{aligned}$$

Now defining the $C_0^{\infty}[-\pi, \pi]$ test function $\varphi(k, k') = g_+^*(k)g_-(k')\langle +|k|-\rangle_{k'}$, we have

$$\begin{aligned} |\langle\psi_+|X(0)|\psi_-\rangle| &= \left| \left\langle \frac{d\delta(k-k')}{d(k-k')} \middle| \varphi(k, k') \right\rangle \right| = \left| \left\langle \delta(k-k') \middle| \frac{d\varphi(k, k')}{d(k-k')} \right\rangle \right| = \\ &= \left| \int_{-\pi}^{\pi} \frac{dk}{2\pi} dk' \delta(k-k') g_+^*(k)g_-(k') \frac{d}{d(k-k')} \langle +|k|-\rangle_{k'} \right| = \\ &= \left| \int_{-\pi}^{\pi} \frac{dk}{2\pi} g_+^*(k)g_-(k)f(k) \right| \leq \max_{k \in [-\pi, \pi]} |f(k)| = f(0) \\ f(k) &:= \frac{n}{\sin^2 \omega}, \quad f(0) = \frac{\sqrt{1-m^2}}{m^2}. \end{aligned}$$

which finally gives

$$|x_{\psi}^{\text{int}}(t)| \leq \frac{2}{m} + \frac{2}{m^2}. \quad (\text{A1})$$

-
- [1] G. M. D'Ariano, Phys. Lett. A **376** (2011).
[2] A. Bisio, G. D'Ariano, and A. Tosini, arXiv preprint arXiv:1212.2839 (2012).
[3] J. von Neumann, *Theory of self-reproducing automata* (University of Illinois Press, Urbana and London, 1966).
[4] S. Wolfram, *A new kind of science*, vol. 5 (Wolfram media Champaign, 2002).
[5] T. Toffoli and N. Margolus, *Cellular automata machines* (MIT press, 1987).
[6] F. Berto and J. Tagliabue, in *The Stanford Encyclopedia of Philosophy*, edited by E. N. Zalta (2012), summer 2012 ed.
[7] A. Ambainis, E. Bach, A. Nayak, A. Vishwanath, and J. Watrous, in *Proceedings of the thirty-third annual ACM symposium on Theory of computing* (ACM, 2001), pp. 37–49.
[8] R. P. Feynman, A. R. Hibbs, and D. F. Styer, *Quantum mechanics and path integrals*, vol. 2 (McGraw-Hill New York, 1965).
[9] R. Feynman, International journal of theoretical physics **21**, 467 (1982).
[10] B. Schumacher and R. Werner, Arxiv preprint quant-ph/0405174 (2004).
[11] P. Arrighi, V. Nesme, and R. Werner, Journal of Computer and System Sciences **77**, 372 (2011).
[12] D. Gross, V. Nesme, H. Vogts, and R. Werner, Communications in Mathematical Physics pp. 1–36 (2012).
[13] P. Knight, E. Roldán, and J. Sipe, journal of modern optics **51**, 1761 (2004).
[14] G. Valcárcel, E. Roldán, and A. Romanelli, New Journal of Physics **12**, 123022 (2010).
[15] A. Ahlbrecht, H. Vogts, A. Werner, and R. Werner, Journal of Mathematical Physics **52**, 042201 (2011).
[16] D. Reitzner, D. Nagaš, and V. Bužek, Acta Physica Slovaca. Reviews and Tutorials **61**, 603 (2011).
[17] T. Nakamura, Journal of mathematical physics **32**, 457 (1991).
[18] I. Bialynicki-Birula, Physical Review D **49**, 6920 (1994).
[19] D. Meyer, Journal of Statistical Physics **85**, 551 (1996).
[20] J. Yepez, Quantum Information Processing **4**, 471 (2006).
[21] J. Magueijo and L. Smolin, Physical Review D **67**, 044017 (2003).
[22] Amelino-Camelia, Int. Journ. of Modern Physics D **11**, 35 (2002).
[23] G. Amelino-Camelia and T. Piran, Physical Review D **64**, 036005 (2001).
[24] K. Huang, American Journal of Physics **20**, 479 (1952).
[25] F. Cannata and L. Ferrari, Physical Review B **44**, 8599 (1991).
[26] L. Ferrari and G. Russo, Physical Review B **42**, 7454 (1990).
[27] F. Cannata, L. Ferrari, and G. Russo, Solid State Communications **74**, 309 (1990).
[28] D. Lurié and S. Cremer, Physica **50**, 224 (1970).
[29] S.-Q. Shen, Phys. Rev. Lett. **95**, 187203 (2005).
[30] E. Bernardes, J. Schliemann, M. Lee, J. C. Egues, and D. Loss, Phys. Rev. Lett. **99**, 076603 (2007).
[31] L. Lamata, J. León, T. Schätz, and E. Solano, Physical review letters **98**, 253005 (2007).
[32] R. Gerritsma, G. Kirchmair, F. Zähringer, E. Solano,

- R. Blatt, and C. Roos, Nature **463**, 68 (2010).
- [33] J. Cserti and G. Dávid, Physical Review B **74**, 172305 (2006).
 - [34] T. M. Rusin and W. Zawadzki, Physical Review B **76**, 195439 (2007).
 - [35] J. Schliemann, D. Loss, and R. Westervelt, Physical review letters **94**, 206801 (2005).
 - [36] W. Zawadzki, Physical Review B **72**, 085217 (2005).
 - [37] W. Zawadzki and T. Rusin, Physics Letters A **374**, 3533 (2010).
 - [38] A. Geim and K. Novoselov, Nature materials **6**, 183 (2007).
 - [39] W. Zawadzki and T. Rusin, Journal of Physics: Condensed Matter **23**, 143201 (2011).
 - [40] J. Vaishnav and C. Clark, Physical review letters **100**, 153002 (2008).
 - [41] X. Zhang, Phys. Rev. Lett. **100**, 113903 (2008).
 - [42] M. I. Katsnelson and K. Novoselov, Solid State Communications **143**, 3 (2007).
 - [43] L. Sansoni, F. Sciarrino, G. Vallone, P. Mataloni, A. Crespi, R. Ramponi, and R. Osellame, Physical review letters **108**, 010502 (2012).
 - [44] E. Schrödinger, *Über die kräftefreie Bewegung in der relativistischen Quantenmechanik* (Akademie der wissenschaften in kommission bei W. de Gruyter u. Company, 1930).
 - [45] J. A. Lock, Am. J. Phys **47**, I979 (1979).
 - [46] P. Kurzyński, Physics Letters A **372**, 6125 (2008).
 - [47] D. A. Meyer, International Journal of Modern Physics C **8**, 717 (1997).
 - [48] G. M. D'Ariano and P. Perinotti, unpublished (2013).
 - [49] The interactions between cells in the interpolation interval would be nonlocal, and, in addition, the Hamiltonian would involve distant cells.